High-resolution tSZ observations of a large sample of clusters of galaxies

P.I.: Frédéric Mayet & Barbara Comis (LPSC Grenoble)

1 Scientific Rationale

As the largest gravitationally collapsed objects in the Universe, clusters of galaxies represent the last step of the hierarchical gravitational process of structure formation. Therefore their abundance in mass and redshift is a powerful cosmological probe, which is sensitive to the primordial density fluctuations, matter contents of the Universe and its whole expansion history.

In a cluster, most of the baryons are present within a gas that is hot (10^6 - 10^8 K), diffuse and completely ionized. It is referred to as the Intra-Cluster Medium (ICM). Cosmic Microwave Background (CMB) photons may interact, through their path toward us, with the free hot electrons in the ICM, being then shifted to higher energies. This interaction, known as the thermal Sunyaev-Zel'dovich (tSZ) effect, results in a CMB flux decrement (increment) at frequencies below (above) 217 GHz, which corresponds to a distortion of the CMB blackbody spectrum. The amplitude of the effect is proportional to the integral of the pressure of the electron population along the line of sight ($y \propto \int P_e \, dl$). Measuring the distribution of the tSZ signal in clusters directly probes the distribution of thermal pressure within the ICM. Furthermore, being a CMB spectral distortion, the tSZ flux is not affected by redshift cosmic dilution. Thus, the tSZ effect represents a particularly well-suited observable to detect and study clusters at high redshift ($z > 0.4$), where their number and distribution is the most sensitive to the underlying cosmology [1].

In the last few years, technological progresses have made possible to detect the tSZ effect routinely. As a consequence, tSZ-selected cluster catalogues containing several thousands of candidates have finally been produced, at arcmin resolution, by the South Pole Telescope (SPT, FWHM $\sim$ 1.1 arcmin at 150 GHz, [2, 3]), the Atacama Cosmology Telescope (ACT, FWHM $\sim$ 1.4 arcmin at 148 GHz, [4]), andprop-IRAM.tex the Planck satellite (FWHM $\sim$ 10 arcmin for tSZ, [5]). ICM observables, such as the tSZ flux, can provide a powerful tool for cosmological investigation with clusters, as long as we are able to convert them into robust mass estimates. In fact, at present, the systematic uncertainties affecting the mass-observable scaling relations represent the limit for cluster-derived cosmological constraints. Planck, ACT and SPT have detected many clusters through tSZ performing a blind survey able to use this effect to identify objects not yet discovered at other wavelengths. However, their relatively limited resolution ($\gtrsim$ 1 arcmin) only allows detailed study of the spatial distribution of the signal for low redshift clusters. The use of tSZ-selected cluster samples for cosmological purposes now requires an accurate understanding of the astrophysical systematics affecting the baryonic proxies (i.e. the tSZ integrated flux, Y) of the cluster total mass (M_{tot}), in particular at high-z. In this context, measurements reaching sub-arcminute angular resolution for cluster pressure profiles are a mandatory step for precise cluster and tSZ cosmology, since they will contribute to improve our knowledge of the statistical properties of galaxy cluster structure reducing the related uncertainties and biases, which now limit cosmological studies [6].

Such measurements can only be made possible by high sensitivity and high spatial resolution tSZ observations. The NIKA2 camera at the IRAM 30 m telescope is the only instrument currently in operation that is suited for this kind of observations and follow-ups, given its resolution, sensitivity and dual-band observation capability. Conducting sub-arcminute tSZ observations of a representative population of clusters across the little explored redshift range $0.5 \lesssim z \lesssim 0.9$ will bring detailed insight of the properties of clusters over more than 3 Gyr. This will allow us to understand the processes driving the physical evolution of massive halos in the Universe and to quantify how the cluster thermal content and distribution evolves as massive halos continue to grow through accretion and merging processes. This will result in a better characterization of the mass-observable scaling relations together with its potential evolution with redshift across a redshift range relevant for cosmology, which, in turn, will have implications on the precision of the cosmological constraints from any tSZ-selected cluster survey. In short, the proposed LP sample will enable a major breakthrough in the use of clusters of galaxies for cosmological studies.

2 Immediate Objective

The main objective of this program is to obtain *high resolution* tSZ observations for a sample of objects, which are *representative* of the population of clusters of galaxies, at *intermediate and high redshifts ($z > 0.5$)* and spanning

more than an order of magnitude in SZ signal and mass. These observations will be used for an in-depth study of the evolution of cluster physical properties across cosmic times. At present, cluster and tSZ derived cosmological constraints are limited by our incomplete understanding of the impact of the details of cluster astrophysics. Thus, this study is mandatory to handle systematics and achieve precision cosmology with clusters. Our primary objective is to produce unprecendented high-quality deliverables, such as tSZ maps and pressure profiles (see. Fig. 1) for the selected cluster sample that we will exploit and release to the cosmology and astrophysic communities.

More precisely we aim at:

i) Exploring and test the regularity of the cluster pressure profile at $z > 0.5$, following the approach that has been used in X-rays with the REXCESS sample at $z < 0.2$ [7], but with an observable (the SZ signal) that probes directly the ICM pressure. The major issue is the study of the mass-observable scaling relation and its evolution with the redshift and the cluster dynamical state.

ii) Detecting the presence of sub-structures (e.g. secondary peaks, deviations from spherical symmetry, overall irregular shape), their significance and impact on the mass estimates via the mass-observable relation.

iii) Introducing, defining and testing parameters that allow us to quantify the cluster dynamical state through its tSZ morphology. A robust tSZ-defined indicator of cluster morphology would permit to study the disturbed cluster fraction as a function of redshift and would represent a useful tool to explore its correlation with deviation from the cluster self-similar behavior observed at low z and in simulations for both the pressure profile and scaling laws.

iv) Studying the correlation between the SZ indicator(s) of cluster dynamical state, the dispersion around the average cluster pressure profile and its evolution with redshift and radial scale.

3 Feasibility and Technical Justification

The NIKA2 camera represents a technological breakthrough for high-resolution observations of the tSZ effect from cluster of galaxies:

– It *operates simultaneously at two frequency* bands, 150 and 260 GHz, at which tSZ shows up respectively as a negative and a slighlty positive distortion of the CMB spectrum, producing a very distinctive cluster signal on the observed maps. With NIKA, we have shown that dual-band observations can be used to remove the atmospheric noise without affecting the signal, taking advantage of the characteristic tSZ spectrum, see [8, 9, 10, 11, 12]. Both small and large angular scales may then be recovered. In addition they are of the outmost interest to detect foreground contaminating sources, and account for their flux.

– NIKA2 is made of *arrays of thousands of high sensitive* Kinetic Inductance Detectors (*KIDs*). In particular we expect a sensitivity in Compton parameter units of $\sim 10^{-4}$ per hour and per beam. This should allow us to obtain reliable tSZ detections and mapping of clusters of galaxies in few hours.

– NIKA2, *coupled to the IRAM 30 m telescope* allows us to map clusters of galaxies to a *resolution of typically* 20 arcsec *within a* 6.5 arcmin *diameter FOV*.

NIKA2 tSZ capabilities have been demonstrated through a pilot study conducted with its pathfinder, NIKA. In the context of this pilot study, in order to validate the KIDs capabilities when dealing with such a faint and diffuse signal, we have mapped the tSZ in the direction of six clusters of galaxies: **i)** RX J1347.5-1145, an intermediate redshift object ($z = 0.45$), which has been the perfect target for the first tSZ detection ever achieved with KIDs [8]; **ii)** CL J1226.9+3332, a very high redshift cluster, $z = 0.89$ [9], **iii)** MACS J0717.5+3745, which has been used to report the first model-independent mapping of the kinetic Sunyaev-Zel'dovich [10]; **iv)** MACS J1423.9+2404, a relaxed cluster, which has been used to explore the impact of the presence of foreground radio and IR sources and how to deal with them in the data reduction [11]; **v)** PSZ1 G046.13+30.75 and PSZ1 G045.85+57.71, two Planck-discovered clusters (at $z = 0.57$ and $z = 0.61$, respectively) chosen to test NIKA2 capabilities at the level of detection of the Planck catalogue of tSZ sources [12]. We have successfully explored a wide range of cluster morphologies and amplitudes of the tSZ flux.

To date, the Mustang and Bolocam instruments (at the focus of the Green Bank Telescope and of the Caltech Submillimeter Observatory, respectively) have also produced scientific quality tSZ observations. They are expected to be followed by next generation instruments, Mustang-2 and BolocamII, which represent the closest NIKA2 concurrent instruments. However, none of them will be operational before NIKA2 and none of them will combine sufficiently large FOV and high angular resolution to carry out the project described here. As an alternative to large diameter telescopes, interferometers can reach very high angular resolution, but they cannot recover the large scale signal and they are time expensive.

Target selection – Our target selection strategy is mainly driven by the need of selecting *a sample of objects that is representative of the cluster population*. A representative sample, i. e. which is not biased towards a given cluster morphology, will allow us *to derive mass-observable scaling relations that can be applicable to the whole cluster population* (not only relaxed or unrelaxed ICM) and *to achieve a global characterization of clusters and an improved control of systematics due to their astrophysics*. A flux-selected subset of a tSZ-selected cluster catalogue fulfills the requirement of a representative sample. This criterion follows the approach adopted to build the REXCESS sample, an XMM-Newton large program dedicated to the in-depth study of a representative sample of 33 clusters ($0.055 < z < 0.183$). This sample has been used to build the universal pressure profile for the ICM [7], an average profile for the cluster population, derived from observations, scaled by mass and redshift according to the standard self-similar model. The LP SZ sample can be used to continue the REXCESS-enabled characterisation of the cluster statistical properties, further pushing the assessment of the potential evolution of the pressure profile to higher redshifts.

In order to fulfill our goal with NIKA2, we consider the following main target selection criteria:

– clusters belonging to tSZ-selected samples (already existing tSZ based cluster samples from Planck and ACT), for which the redshift information is available;

– $0.5 < z < 0.9$, to explore the cluster statistical properties beyond the local Universe;

– dec > -11, to ensure observability of the sources from the Pico Veleta site.

We have used the above criteria and the Planck and ACT cluster samples to select a representative sample of clusters of galaxies suitable for our purposes. We note however that the follow-up of the tSZ-discovered-Planck clusters is not yet fully completed. We consider **two bins in redshift ($0.5 < z \leq 0.7$ and $0.7 < z \leq 0.9$)**, and for each of them, we have defined **five bins in $E_z^{-2/3} D_A^2 Y_{500}$** (Fig. 2, bottom panel), which is the quantity related to the cluster mass M_{500} through the scaling relation we aim at calibrating (D_A is the angular diameter distance and $E_z = H(z)/H_0$ accounts for the background universe evolution). Within each mass bin we have selected five clusters randomly, giving preference to those that have been selected also for an on-going XMM large program (P.I.: M. Arnaud). The selected sample is listed in Tab. 1. For the two largest $E_z^{-2/3} D_A^2 Y_{500}$ bins (massive clusters) at high redshift we have at present only 4 and 1 cluster respectively. In summary we have selected 45 out of 50 clusters. In agreement with IRAM the remaining five clusters will be defined within one year from the starting of the large program. For this we will take advantage of the information provided by current and near-future Planck and ACT follow-up programs, which are expected to populate the $z > 0.6$ region. In addition, we have selected two spare clusters at high redshift as indicated in by the last two rows of Table 1. The reason for this is the large uncertainties in the definition of the properties of high redshift clusters.

Observing strategy and data reduction –

Based on the experience with the NIKA camera, we will perform OnTheFly (OTF) scans in right ascension and declination. We will alternate different orientations of the scans (e.g. 0, 45, 90,-45 degrees) and perform scans of 13' × 8' (more than one third of the observing time will be spent on the core of the signal) so that we reach cluster outskirts (roughly up to twice the characteristic radius of the cluster r_{500}) even for the lowest redshift clusters. This will allow us to properly define the zero level of the final map and measure angular scales structures up to the scan size. To estimate the expected cluster signal in the maps we use the Y_{500} ($Y_{500} = \int_{\Omega_{r_{500}}} y d\Omega$), M_{500} and redshift provided from the latest updated version of Planck and the ACT cluster catalogs. We then consider an universal pressure profile [7] to model the distribution of the signal around the cluster center for each given Y_{500}. The required observation time are optimized cluster by cluster, in order to obtain an homogeneous sample in terms of signal to noise at a given characteristic radius θ_{500} (radius at which the cluster mean over density is equal to 500 times the critical density of the Universe). We impose at least a 1-σ measurement of the cluster pressure profile at θ_{500} (see. Fig. 1) for all clusters in the sample. Notice that the θ_{500} is computed from the redshift and the tSZ-derived M_{500} reported in the catalogues, in order to have a homogeneous definition that only depends on the tSZ flux and the cluster distance.

Transforming the above criteria into a rms noise in the map we compute the observing time per cluster using the NIKA2 time estimator provided by IRAM. We consider millimetre weather conditions (2 mm of pwv), an overhead factor of two, 60 % of valid detectors and a conservative filtering of about 30 % within the cluster characteristic radius. The expected observing time per cluster are presented in Table 1. Roughly speaking we require observing times of about 10 to 30 hours for the lightest clusters and of 1-3 hours for the most massive ones. For the 45 selected clusters we obtain a total observing time of 280 hours. The remaining 20 hours will be used to accommodate the observations of the lacking five high mass clusters. In the case of improved instrument performance we intend to keep the same number of sources and the same integration time for each of them. In particular in the case of goal

performance we will extend morphology analysis out to the cluster outskirts.

In terms of data reduction we will use the tSZ dedicated pipeline developed for the NIKA experiment. This pipeline has beed intensively tested using the NIKA data and was used for the NIKA SZ publications [8, 9, 10, 11, 12]. Needed improvements and updates will be directly carried out by our team that led the analysis of the NIKA SZ data. NIKA2 will be able to observe simultaneously at two wavelengths allowing for self consistent foreground source subtraction (e.g. [11]). However NOEMA could be eventually used to obtain complementary information in this sense, requiring reasonable observing times.

4 Organizational Issues

Project management – For this project we have gathered a highly experienced team with a large expertise in submillimetre observations, data reduction and tSZ science as well as complementary external observations. A project PI (F. Mayet) and a co-PI (B. Comis) will coordinate the different activities. As an expert of the NIKA2 pipeline, the co-PI is in charge of coordinating the data reduction, according to NIKA2 collaboration rules. The SZLP team have a long experience of SZ data with NIKA observations, together with external data for joint analysis. For the sake of clarity, the team can be presented in two sub-teams:

- SZLP analysis team : R. Adam, B. Comis, M. De Petris, J.-F. Macias Perez, F. Mayet, L. Perotto, C. Romero, F. Ruppin.
The SZLP analysis team has developped a SZ pipeline enabling the processing from raw data to SZ maps and pressure profiles (Fig. 1), which are the main deliverables of this Large Project. It has been tested and optimized on observation with the NIKA intrument, leading to five papers in the recent years [8, 9, 10, 11, 12].
- SZLP ancillary data team : M. Arnaud, I. Bartalucci, G. Pratt, E. Pointecouteau (XMM group for X-rays), J. A. Rubino Martin, R. Barrena Delgado (GTC team for optical observations) and C. Ferrari (LOFAR team for radio emission).
Experts of external data have contributed to the definition of the cluster sample. Furthermore, to maximize the scientific output of the NIKA2 SZLP, they are participating in the joint analysis with NIKA2 data. Also, follow-ups are being prepared for the near future. Note that this team has contributed to the NIKA SZ papers, proving the added value of external data [8, 9, 10, 11, 12].

Data policy and deliverables– The project data and products will be made publicly available by the NIKA2 collaboration in a dedicated database after the end of the LP observations, following the standard IRAM rules. These products will consist of the raw data, the calibrated map per cluster and associated processing information, and pressure profiles per cluster.

Complementary external data – The scientific output of the NIKA2 LP could be enriched by the use of high quality external data at other wavelengths or with other probes. Other than the use of publicly available data, formal collaborations are being established to collect extra proprietary data. At this regard, XMM data from a companion X-ray follow-up of high-redshift clusters will be used. With NIKA2 the cluster gas will be finally mapped in tSZ with a quality (in terms of sensitivity and angular resolution) comparable to X-ray, even for intermediate and high-redshift clusters. Thus, the natural combination of these two direct observables of the intra-cluster hot gas will allow us to estimate the total masses (under the assumption of hydrostatic equilibrium) as well as a full physical characterization of the (radial) distribution of the cluster thermodynamic properties: not only pressure, but also temperature ($T_e(r) \propto P_e(r)/n_e(r)$) and entropy ($K(r) \propto P_e(r)n_e^{-5/3}$) which are essential to unveil cluster thermodynamic history. Indeed, the tSZ signal directly probes the gas pressure, while X-ray data deliver the gas density squared and temperature. The different dependencies of tSZ and X on the electron density will also provide a powerful probe of gas clumping, and an improved insight on the cluster tridimensional shape.

Furthermore, optical follow-ups could be performed for a large number of the NIKA2 clusters using the GTC (Gran Telescopio Canarias) imaging and spectroscopy facilities. The combination of tSZ and X-ray data to optical/NIR observations of the cluster galaxies will further help to investigate the connection between galaxy properties (luminosity function, SFR, stellar mass) and those of the ICM, and thereby bring constraints on feedback mechanisms at play within clusters. Moreover, weak lensing measurements will provide complementary measurements of the dark matter distribution and total mass of the clusters, in a totally independent way, then affected by different systematics. Optical mass estimate are not based on the same assumptions.

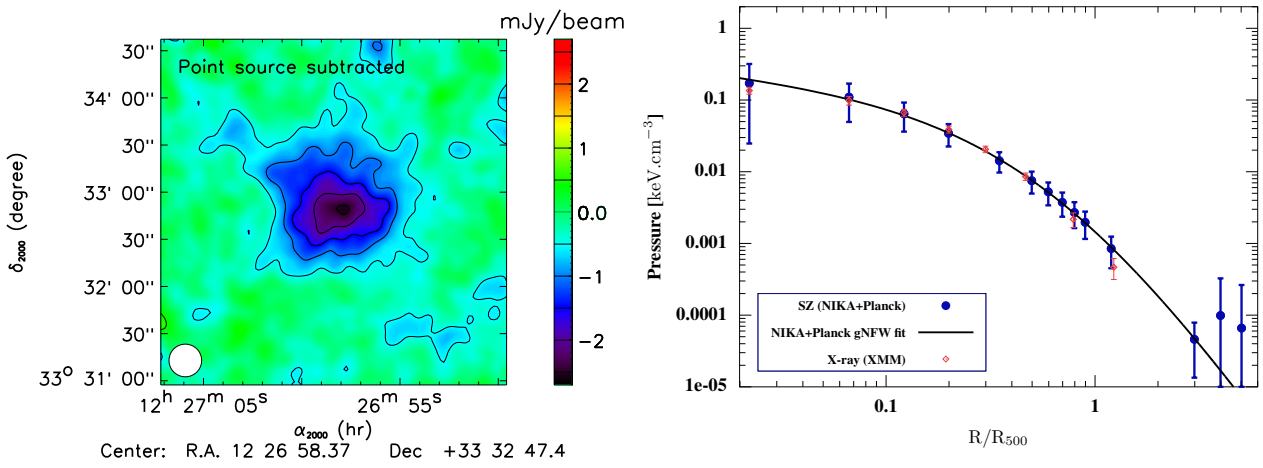

Figure 1: **Left:** NIKA map of CL J1226.9+3332 at 150 GHz [9]. The effective beam FWHM (18.2 arcsec native resolution plus an extra 10 arcsec FWHM Gaussian) is shown as the bottom left white circle. The overall effective observing time on the cluster is 7.8 hours and $\theta_{500} \sim 2$ arcmin for this cluster. **Right:** Non-parametric pressure profile (blue) deprojected from the NIKA tSZ surface brightness map of a Planck-discovered cluster (PSZ1 G045.85+57.71) observed with NIKA in Oct. 2014. Fig. from [12]. This was part of a NIKA pilot study aimed at optimising the treatment of the NIKA2 tSZ Large Programme.

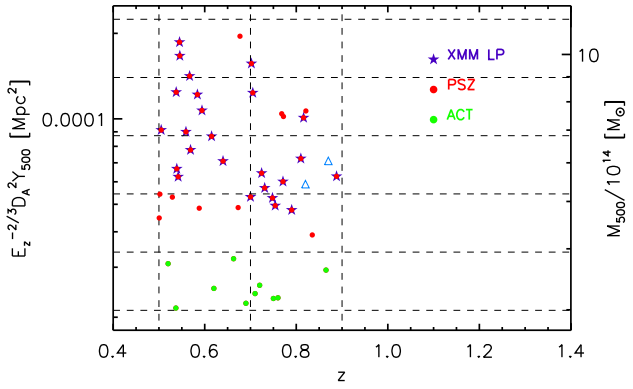

Figure 2: Clusters extracted from the Planck and ACT (equatorial) tSZ-selected samples, in the redshift range we want to explore and observable from the Pico Veleta site (dec > -11). The different symbol used are reported in the legend, the cyan triangles are the two further objects belonging to the XMM large program (listed at the end of Tab. 1). They have not been selected for the NIKA2 sample, but they fulfill our redshift and observability criteria.

References

[1] Carlstrom, J. E., Holder, G. P., & Reese, E. D. 2002, ARA&A, 40, 643

[2] Reichardt, C. L., Stalder, B., Bleem, L. E., et al. 2013, ApJ, 763, 127

[3] Bleem, L. E., Stalder, B., de Haan, T., et al. 2015, ApJS 216, 27

[4] Hasselfield, M., Hilton, M., Marriage, T. A., et al. 2013, J. Cosmology Astropart. Phys., 7, 8

[5] Planck Collaboration, Ade, P. A. R., Aghanim, N., et al. 2014, A&A, 571, A29, ArXiv:1502.01598

[6] Planck Collaboration, Ade, P. A. R., Aghanim, N., et al. 2015, ArXiv:1502.01597, ArXiv:1502.01596

[7] Arnaud, M., Pratt, G. W., Piffaretti, R., et al. 2010, A&A, 517, A92

[8] Adam, R., Comis, B., Macías-Pérez, J.-F. et al. 2014b, A&A, 569, A66

[9] Adam, R., Comis, B., Macías-Pérez, J.-F. et al. 2015, A&A, 576, A12

[10] Adam, R., Bartalucci, I., Pratt G. W. et al. 2016, ArXiv:1606.07721

[11] Adam, R., Comis, B., Bartalucci, I. et al. 2016, A&A, 586, A122

[12] Ruppin, F., Adam, A., Comis, B., et al. 2016, ArXiv:1607.07679, to appear in A& A

Name	Alternative Name	z	θ_{500} [arcmin]	Y_{500} [10^{-4} arcmin^2]	t_{obs} [hr]
ACT-CL J0219.8+0022		0.537	2.169	1.700	17.2
ACT-CL J2152.9-0114		0.690	1.820	1.500	26.8
ACT-CL J0240.0+0116		0.620	2.022	1.800	15.9
ACT-CL J2302.5+0002		0.520	2.381	2.500	7.9
ACT-CL J0223.1-0056		0.663	2.023	2.200	10.8
PSZ2 G081.02+50.57	RMJ153906.4+503644.9	0.501	2.650	3.739	3.3
PSZ2 G106.15+25.75	PSZ1 G106.15+25.76	0.588	2.396	3.573	3.7
PSZ2 G108.27+48.66	PSZ1 G108.26+48.66	0.673	2.185	3.304	4.4
PSZ2 G133.59+50.68	RMJ114649.1+650506.8	0.529	2.626	4.228	2.7
PSZ2 G080.64+64.31	RMJ142716.1+440730.6	0.502	2.741	4.523	2.3
PSZ2 G212.44+63.19	PSZ1 G212.51+63.18, RMJ105252.4+241530.0, WHL J163.208+24.18	0.542	2.663	4.896	2.1
PSZ2 G094.56+51.03	PSZ1 G094.54+51.01, RMJ150822.0+575515.2, WHL J227.050+57.90	0.539	2.706	5.244	1.8
PSZ2 G193.31-46.13	PSZ1 G193.29-46.13, PLCK G193.3-46.1	0.640	2.426	4.957	2.0
PSZ2 G046.13+30.72	PSZ1 G046.13+30.75, RMJ171705.5+240423.6	0.569	2.679	5.868	1.4
PSZ2 G099.86+58.45	PSZ1 G099.84+58.45, WHL J213.697+54.78	0.615	2.589	6.213	1.3
PSZ2 G183.90+42.99	PSZ1 G183.92+42.99, RMJ091051.0+385022.4, WHL J137.713+38.83	0.559	2.788	6.884	1.1
PSZ2 G211.21+38.66	PSZ1 G211.23+38.63, RXC J0911.1+1746, RMJ091111.5+174628.9	0.505	3.008	7.575	1.0
PSZ2 G045.32-38.46	MACSJ2129.4-0741, RMJ212926.1-074127.9, J2129.4-0741	0.594	2.758	7.841	1.0
PSZ2 G144.83+25.11	PSZ1 G144.86+25.09, MACSJ0647.7+7015, RXC J0647.8+7014	0.584	2.859	9.026	1.0
PSZ2 G201.50-27.31	PSZ1 G201.50-27.34, MACSJ0454.1-0300, RXC J0454.1-0300	0.538	3.043	9.783	1.0
PSZ2 G155.27-68.42	PSZ1 G155.25-68.42, RMJ013725.0-082722.7, WHL J24.3324-8.477	0.567	3.002	10.711	1.0
PSZ2 G111.61-45.71	PSZ1 G111.60-45.72, RXC J0018.5+1626, CL 0016+1609	0.546	3.182	12.991	1.0
PSZ2 G228.16+75.20	PSZ1 G228.21+75.20, RXC J1149.5+2224, RMJ114935.7+222354.6, MCS J1149.5+2223	0.545	3.250	14.522	1.0
PSZ2 G209.79+10.23	PSZ1 G209.80+10.23	0.677	2.819	13.220	1.000
ACT-CL J0018.2-0022		0.750	1.739	1.500	27.0
ACT-CL J0058.0+0030		0.760	1.742	1.500	25.0
ACT-CL J2130.1+0045		0.710	1.823	1.600	22.0
ACT-CL J0119.9+0055		0.720	1.825	1.700	20.0
ACT-CL J0215.4+0030		0.865	1.648	1.800	21.0
PSZ2 G104.74+40.42	PSZ1 G104.78+40.45	0.835	1.816	2.417	9.0
PLCK G079.95+46.96		0.790	1.955	3.013	5.6
PSZ2 G088.98+55.07	PSZ1 G089.04+55.07	0.754	2.029	3.178	5.0
PSZ2 G087.39+50.s92	PSZ1 G087.32+50.92, AMF J231.538+54.13	0.748	2.064	3.393	4.3
PSZ2 G097.52+51.70		0.700	2.162	3.530	3.9
PSZ2 G084.10+58.72	PSZ1 G084.04+58.75	0.731	2.128	3.717	3.6
PSZ2 G086.93+53.18	PSZ1 G086.93+53.18, WHL J228.466+52.83	0.771	2.074	3.828	3.5
PSZ2 G160.83+81.66	BVH2007 154, CL J1226.9+3332	0.888	1.907	3.827	3.7
PSZ1 G226.65+28.43	WHL J134.086+1.780	0.724	2.190	4.209	2.8
PLCK G227.99+38.11		0.810	2.079	4.532	2.5
PSZ2 G091.83+26.11	PSZ1 G091.82+26.11	0.816	2.200	6.298	1.3
PSZ1 G140.10+50.09		0.772	2.286	6.486	1.3
PSZ1 G224.73+33.65	CXOMP J091126.6+05	0.768	2.303	6.647	1.2
PSZ2 G141.77+14.19	PSZ1 G141.73+14.22, WHT	0.821	2.214	6.641	1.2
PSZ1 G080.66-57.87	ACT-CL J2327.4-0204	0.705	2.518	8.182	1.0
PSZ2 G138.61-10.84	PSZ1 G138.60-10.85	0.702	2.639	10.395	1.0
PSZ2 G071.82-56.55	*MEGACAM (redshift id)*	*0.870*	*1.978*	*4.358*	*2.3*
PSZ2 G092.69+59.92	*MEGACAM (redshift id)*	*0.820*	*1.984*	*3.669*	*2.0*

Table 1: Clusters selected for the NIKA2 SZ large program. We report the Planck/ACT name of the object, the alternative names, the redshift, θ_{500}, Y_{500} and the estimated time. In italics, we list two backup objects from the XMM large program.